The classical two-dimensional XY model with in-plane magnetic field

M E Gouvêa†, F G Mertens‡, A R Bishop and G M Wysin§

Theoretical Division, Los Alamos National Laboratory, Los Alamos, NM 87545 USA

Abstract. We present analytical and numerical simulation studies on the two-dimensional XY classical ferromagnetic model with weak in-plane magnetic field (the reduced field is $h = 0.05$ and it is applied along the x axis). The structure and dynamics of vortex spin configurations are considered. The simulation data show a strong crossover at $T_c \approx 1.0 \, JS^2$; the data for $T < T_c$ are well interpreted by one- and two-spin wave processes with an additional anomalous central peak at $S_{xx}(q, \omega)$ structure function which is suggested as a contribution from domain walls. The data for $T \gtrsim T_c$ can be interpreted by vortex gas theory. The in-plane data can be compared to recent experiments performed on CoCl$_2$-intercalated into graphite. The $S_{zz}(q, \omega)$ shows unusual behaviour as T is increased to $T \gtrsim 1.2 \, JS^2$ indicating that another phase transition or crossover, related to the out-of-plane spin component, can occur.

1. Introduction

Classical two-dimensional (2D), easy-plane (XY) magnetism has attracted a great deal of attention in recent years. As for other low dimensional systems, the interplay between extended fluctuations and large-amplitude localised excitations has been found to be quite rich. Easy plane symmetry in 2D spin systems is particularly appealing because it admits vortex-like spin configurations and the possibility of a topological vortex-antivortex unbinding transition, as proposed by Kosterlitz and Thouless (1973). Improvements in materials preparation have made available a considerable number of quasi-2D ferro- and antiferromagnetic materials and, consequently, the amount of experimental information on spin dynamics has also increased considerably, making possible a comparison with the detailed theoretical predictions that exist for both the fluctuations and excitations in this model. Many of the materials that have been classified as quasi-2D easy plane include anisotropies that can break the rotational symmetry of the XY plane. José *et al* (1977), using a renormalisation group technique, have studied the phase diagram of the 2D-*planar* mode (i.e., spins restricted to the XY-plane) with in-plane symmetry breaking of degree p. Their conclusion is that the Kosterlitz–Thouless

(KT) phase is suppressed if $p < 4$. We emphasise, however, that a *dynamical* description of 2D-XY models must include the out-of-plane spin component S_z. The inclusion of S_z can lead to additional features beyond by those predicted by José *et al* (1977) including anomalies in S_z correlations (Kawabata and Bishop 1982).

In this work, we will concentrate on 2D-XY ferromagnets with an external magnetic field applied along one of the *in-plane* axes. A magnetic field corresponds to symmetry breaking of degree $p = 1$. At low temperatures, the spins are almost completely aligned along the field and a standard spin wave treatment to two spin-wave processes can be used (section 2) to explain the main features concerning the dynamical behaviour in this low-temperature range. As the temperature is raised, non-linear excitations such as vortices and domain walls have to be incorporated in the description. In § 3, we study, analytically and numerically, the effects due to the applied field on the shape and dynamics of vortices; formation of domain walls is also discussed there. Combined Monte Carlo (MC)–molecular dynamics (MD) numerical simulation studies covering a wide temperature range are presented in section 4. A transition is observed at $T_c \simeq 1.0\,JS^2$ and we discuss separately data obtained at temperatures lower than T_c (section 4.1) and above T_c (section 4.2). A comparison between our results and some recent inelastic neutron experiments performed on intercalated graphite compounds (CoCl$_2$–GIC) with an in-plane magnetic field is also included in section 4. The final conclusions are given in section 5.

2. Spin-wave theory

The 2D-XY model in a magnetic field can be described by the classical Hamiltonian

$$H = -\frac{J}{2} \sum_{m,n} (S^x_{m,n} g^x_{m,n} + S^y_{m,n} g^y_{m,n}) - g\mu_B H \sum_{m,n} S^x_{m,n} \tag{2.1}$$

where the summation is taken over the sites (m, n) of a 2D-square lattice, J is the exchange parameter, $S^\alpha_{m,n}$ are the components of the classical spin vector $S_{m,n} = (S^x_{m,n}, S^y_{m,n}, S^z_{m,n})$ and

$$g^\alpha_{m,n} = S^\alpha_{m,n+1} + S^\alpha_{m,n-1} + S^\alpha_{m+1,n} + S^\alpha_{m-1,n} \tag{2.2}$$

is the sum over the nearest neighbours of each site (m, n).

For the pure XY model (in the absence of a field), it is well known that, besides spin waves, one should consider vortices as essential excitations leading to a topological phase transition at T_c (Kosterlitz and Thouless 1973). It has been shown (Nelson and Fisher 1977, Côté and Griffin 1986) that, for temperatures below T_c, the effect of (bound) vortices can be described as a renormalisation of the spin-wave excitations. In the presence of a magnetic field, the possibility of 2π-domain walls being formed represents an additional complication. However, the energy of a domain wall is proportional to its length (and, also, to the field strength) and it is not very probable that many domain walls will be created at low temperature. If the applied field is sufficiently strong, and at low temperatures (above the 3D ordering temperature but below T_c), we can assume that the spins will be aligned nearly parallel to the field so that a spin-wave theory can be used. In this section, we will ignore both vortices and domain walls, and their interactions with spin waves, assuming that for this temperature range such effects will result in a renormalisation of the spin-wave energy. We will find that the principal

features concerning dynamical spin-correlations may be understood within the spin-wave approximation provided that one includes two-spin-wave processes.

We choose x as the quantisation direction and use the Holstein–Primakoff transformation to express the spin operators as boson operators

$$S^x_{m,n} = S - a^+_{m,n}a_{m,n} \qquad S^+_{m,n} = S^z_{m,n} + \mathrm{i}\,S^y_{m,n} = \sqrt{2S}\,a^+_{m,n}.$$

After a straightforward calculation (for details, see e.g. Heilmann *et al* (1981)), spin-correlation functions can be obtained in the context of the harmonic approximation. For the spatial Fourier transform of yy- and zz-correlation functions, we obtain

$$\langle S^y_q(t)S^y_{-q}\rangle = (S/2)(\rho^+_q + \rho^-_q)^2[n_q \exp(\mathrm{i}\omega_q t) + (n_q + 1)\exp(-\mathrm{i}\omega_q t)], \qquad (2.3a)$$

$$\langle S^z_q(t)S^z_{-q}\rangle = (S/2)(\rho^+_q - \rho^-_q)^2[n_q \exp(\mathrm{i}\omega_q t) + (n_q + 1)\exp(-\mathrm{i}\omega_q t)] \qquad (2.3b)$$

where $n_q = [\exp(\hbar\omega_q/k_{\mathrm{B}}T) - 1]^{-1}$ is the usual boson occupation number, ω_q is the spin-wave energy

$$\omega_q = JS(4 + h)^{1/2}(4 + h - \cos q_x - \cos q_y^{1/2}) \qquad (2.4)$$

$h = g\mu_{\mathrm{B}}H/JS$ is the reduced magnetic field, and ρ^+_q, ρ^-_q are given by

$$\rho^{\pm}_q = \tfrac{1}{2}[(JS/\omega_q)(4 + h - \cos q_x - \cos q_y) \pm 1]^{1/2}. \qquad (2.5)$$

It is easily seen from (2.3), that a sharp one-spin wave peak at $\omega = \pm\,\omega_q$ is expected in $S^{\alpha\alpha}(q, \omega)$, $[\alpha = y, z]$. We can also compute the integrated intensities $I^{\alpha}(q) = \int \mathrm{d}\omega\, S^{\alpha\alpha}(q, \omega)$ and obtain the ratio

$$R(q) = I^y(q)/I^z(q) = (\rho^+_q + \rho^-_q)^2/(\rho^+_q - \rho^-_q)^2 \;(>1). \qquad (2.6)$$

In obtaining (2.6), we took the classical limit of (2.3). We will show in section 4 that these predictions for $S^{\alpha\alpha}(q, \omega)$ $[\alpha = y, z]$ agree well with our numerical simulation data.

For the $S^{xx}(q, t)$ function we have

$$\langle S^x_q(t)S^x_{-q}\rangle = \delta_{q,0}\langle (S - \langle a^+_{m,n}a_{m,n}\rangle)\rangle^2\langle\delta S_q(t)\delta S_q\rangle \qquad (2.7)$$

where

$$\langle\delta S_q(t)\delta S_{-q}\rangle = N^{-2}\sum_{q_1,q_2}\delta_{q_1+q_2+q,0}[\![(\rho^+_{q_1}\rho^+_{q_2} + \rho^-_{q_1}\rho^-_{q_2})^2 n_{q_1}(1 + n_{q_2})$$

$$\times \exp[\mathrm{i}(\omega_{q_1} - \omega_{q_2})t] + \tfrac{1}{2}(\rho^+_{q_1}\rho^-_{q_2} + \rho^+_{q_2}\rho^-_{q_1})^2$$

$$\times \{n_{q_1}n_{q_2}\exp[\mathrm{i}(\omega_{q_1} + \omega_{q_2})t] + (1 + n_{q_1})(1 + n_{q_2})$$

$$\times \exp[-\mathrm{i}(\omega_{q_1} + \omega_{q_2})t]\}]\!] \qquad (2.8)$$

is due to the spin fluctuations. The first term in (2.7) gives a Bragg peak while the second term, defined by (2.8), is the contribution due to two-spin wave processes: the first term in (2.8) corresponds to the simultaneous creation and annihilation of spin waves while the second term represents the two-spin wave annihilation $(n_{q_1}n_{q_2})$ and creation

$[(1 + n_{q_1})(1 + n_{q_2})]$ processes—we shall focus only on the creation process. Taking the classical limit and the temporal Fourier transform of each term in (2.8), we have

$$G_D^{xx}(q, \omega_D) = \frac{1}{4\pi N} \sum_{q_1} \frac{T^2}{\omega_{q_1} \omega_{q+q_2}} (\rho_{q_1}^+ \rho_{q+q_1}^+ + \rho_{q_1}^- \rho_{q+q_1}^-)^2 \left| \frac{\partial}{\partial q'} (\omega_{q+q'} - \omega_{q'}) \right|^{-1} \qquad (2.9)$$

for the first term, and

$$G_S^{xx}(q, \omega_S) = \frac{1}{4\pi N} \sum_{q_2} \frac{T^2}{\omega_{q_2} \omega_{q+q_2}} (\rho_{q_2}^+ \rho_{q+q_2}^- + \rho_{q_2}^+ \rho_{q+q_2}^-)^2 \left| \frac{\partial}{\partial q'} (\omega_{q+q'} + \omega_{q'}) \right|^{-1} \qquad (2.10)$$

for the two-spin wave creation where q_1 and q_2 are restricted by the conditions

$$\omega_D = \omega_{q+q_1} - \omega_{q_1} \qquad \omega_S = \omega_{q+q_2} + \omega_{q_2}. \qquad (2.11)$$

The subscripts D and S stand for difference and sum processes as suggested by (2.11). We can expect a very complicated spectrum because there is a singularity in $G_\alpha^{xx}(q, \omega_\alpha)$ ($\alpha = D, S$) for each critical point of $\omega_{q+q'} \pm \omega_{q'}$ as a function of q'. In order to obtain some information about the spectrum, we consider small values for the wavevector q so that an expansion can be made and we obtain, approximately,

$$\omega_D \simeq \omega_{q_1} q \sin q_{1x} / [4 + h - 2(\cos q_{1x} + \cos q_{1y})] \qquad (2.12)$$

$$\omega_S \simeq \omega_{q_2}\{2 + q \sin q_{2x} / [4 + h - 2(\cos q_{2x} + \cos q_{2y})]\}. \qquad (2.13)$$

(In order to obtain (2.12) and (2.13), we imposed the condition that the q vector must lie along the x-axis.) Even with all these approximations, it is not an easy task to perform the sums indicated in (2.9) and (2.10), but for $q = 0$ we can say that the difference and sum peaks will occur at $\omega_D = 0$ and $\omega_S = 2JS(h^2 + 6h + 4)^{1/2}$; for $q \neq 0$, we expect these frequency peaks to change (approximately) linearly with $|q|$. These predictions will be checked by the numerical simulation data (section 4).

3. Vortices in a magnetic field

The spin vector S can be described by two continuously varying fields, $\Theta(r, t)$ and $\Phi(r, t)$, as

$$S(r, t) = S(\cos \Theta(r, t) \cos \Phi(r, t), \cos \Theta(r, t) \sin \Phi(r, t), \sin \Theta(r, t)) \qquad (3.1)$$

and, then, the continuum equations of motion corresponding to Hamiltonian (2.1) can be obtained. A general solution to these equations of motion is not available. A non-trivial *static* ($\Theta = 0$) solution can be obtained by solving the sine–Gordon equation

$$\nabla^2 \Phi = h \sin \Phi. \qquad (3.2)$$

In the absence of any field, this equation gives the well-known planar vortices of the *XY* model

$$\Theta_0 = 0 \qquad \Phi_0 = \varphi + c \qquad (h = 0) \qquad (3.3)$$

where φ is a polar coordinate, and c is an arbitrary constant. An analytical solution to (3.2), for $h \neq 0$, was given by Hudák (1982), but it corresponds to a vortex with vorticity 4, which is not expected to play an important role in dynamics (Amit *et al* 1980). In order

to study the modifications to the static vortex shape (specified by (3.3)) due to a *weak* applied field, we will adopt an approximate perturbative treatment inserting

$$\Phi = \Phi_0 + \Phi_1 \qquad \Theta = \Theta_0 + \Theta_1 \tag{3.4}$$

and

$$\dot{\Phi} = - \boldsymbol{v} \cdot \boldsymbol{\nabla}\Phi \qquad \dot{\Theta} = - \boldsymbol{v} \cdot \boldsymbol{\nabla}\Theta \tag{3.5}$$

into the equations of motion. Here, Φ_0 and Θ_0 are given by (3.3) and $\boldsymbol{v}$ is the vortex velocity.

This procedure is straightforward and was previously used by the authors (Gouvêa *et al* 1989a) to study the distortion suffered by a vortex due to the movement induced by interactions with other vortices in the system. After linearising in Θ_1, Φ_1 and $\boldsymbol{v}$, we obtain

$$\Theta_1 \simeq (v/4JS)(\sin(\varphi - \alpha)/r) \qquad (r \to \infty) \tag{3.6a}$$

where α is the angle between $\boldsymbol{v}$ and the x-axis, and

$$\Phi_1 = - (hr^2/3) \sin(\varphi + c) \tag{3.6b}$$

where h is considered as a small parameter (in our numerical simulations, section 4, we used $h = 0.05$). The asymptotic solution for Θ_1, equation (3.6a) is asymmetric about $\boldsymbol{v}$—the out-of-plane component has different signs on each side of the line along which the vortex moves. This result is identical to the one found for 2D-XY systems (Gouvêa *et al* 1989a). The deformation of the in-plane field, Φ_1, forces the spins into the direction of the magnetic field, i.e., the effect of the magnetic field is to create a region (domain) where all spins lie along the $+x$ direction: as the size of this region increases, the vortex is pushed to one of the system's boundaries. It should be noted that Φ_1 and, also, the direction of motion depend on the constant c. In the pure XY-model, this constant has no role and is often ignored. However, when a certain in-plane magnetic field is applied, the value of c directly influences the static force F_H due to interactions with the field and, consequently, the direction of motion α. These conclusions can also be drawn from Huber's (1982) expression for F_H.

At low temperature, we are concerned with vortex–antivortex *pairs* (Kosterlitz and Thouless 1973). In the absence of a field, the energy of a pair does not depend on the value of the constant c (3.3) of each one of the pair's components. A field breaks the rotational symmetry of the XY-plane and then different pairs (corresponding to different cs) will have different energies; one can easily estimate which combinations correspond to low or high energy simply by trying to put together different vortices and antivortices (neglecting any distortions) and by counting the number of spins (in fact, spin components) aligned parallel or antiparallel to the field. The interesting conclusion is that the configurations that lead to minimal energy have lower energy for $h \neq 0$ than for $h = 0$. This means that these energetically favoured pairs will be more tightly bound and will require more energy to unbind. Consequently, we can expect that, for $h \neq 0$, vortex-antivortex pairs will unwind at a temperature higher than T_{KT} ($\approx 0.8\,JS^2$).

In order to check the approximate analytical results given by (3.6) and to get information on how the discreteness of the lattice affects the vortex motion, simulation studies
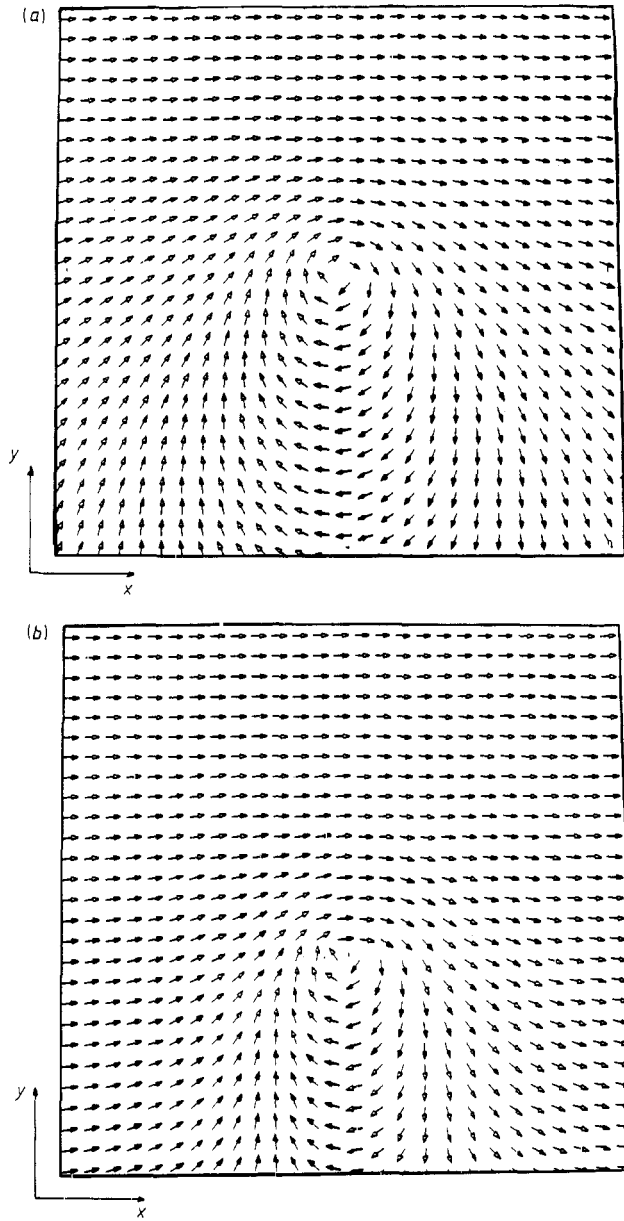
Figure 1. A single vortex in a magnetic field at (a) $t = 6.0$ and (b) $t = 15.0$ time units, starting from a planar vortex ($\Theta = 0$, $\Phi = \varphi + \pi/2$). Black and white arrows denote positive and negative out-of-plane spin components, respectively. The vortex moves along the y direction. Only a segment of the 40×40 simulated lattice is shown.

were performed on a 40×40 square lattice. The discrete equations of motion used in the numerical simulations are

$$\dot{S}_i = S_i \times F_i - \varepsilon S_i \times (S_i \times F_i) \tag{3.7}$$

$$F_i = J \sum_j [(S_j^x + h)\hat{e}_x + S_j^y \hat{e}_y + S_j^z \hat{e}_z]. \tag{3.8}$$

The sum on j only runs over the nearest neighbours of i. The parameter ε is the strength of a Landau–Gilbert damping, which was included to damp out spin waves generated from non-ideal initial conditions. A single planar ($\Theta = 0$) vortex (with $c = -\pi/2$) centred in a unit cell of the lattice was used as the initial condition. The equations for the xyz-spin components were integrated using a fourth-order, Runge–Kutta scheme with time step 0.04 (in time units h/JS). Neumann boundary conditions and a damping strength $\varepsilon = 0.1$ were used.

Figures 1(a) and 1(b) show the instantaneous configuration at times $t = 6.0$ and 15.0. From figure 1(a) we see that the vortex moves along the $-y$ direction with the out-of-plane spin components having different signs (white and black arrows) on each side of the y axis. It can also be seen that the distortion of the in-plane spin component agrees, qualitatively, with (3.6b). Figure 1(b), at a later time, shows a large domain with all spins aligned along the field; the vortex is being pushed to the opposite boundary as this domain increases. The single vortex, which, initially ($t = 0$), extended itself through the whole system, is now restricted to a much smaller region. The structure seen in figure 1(b) can be described as a vortex whose radius corresponds to a few lattice constants ($\sim 4a$) bound to 2π-domain wall. This 2π-domain wall consists of *two* π-domain walls separated by (approximately) the vortex diameter, and its length L is the distance that separates the vortex from the boundary to which it is moving. The energy of a domain wall increases linearly with L, and in an infinitely extended system, the energy of the structure shown in figure 1(b) would diverge as $L \to \infty$ so that we should not expect to find these structures at low temperatures. However, vortex-antivortex pairs bound by domain walls have finite energy and can be nucleated giving rise to a *linear* interaction potential between vortices.

Entropy arguments (Lee and Grinstein 1985, Einhorn *et al* 1980, Tang and Mahanti 1986) can be used to determine the phase diagram. Basically, we should concentrate on two characteristic temperatures T_1 and T_2. The free energy related to domain walls involves a competition between two terms with the same functional dependence since both the energy *and* the entropy of a domain wall depend *linearly* on L. T_1 corresponds to the temperature at which these terms give the same contribution; for $T \geqslant T_1$, the walls connecting vortex-antivortex pairs become flexible (i.e., transverse fluctuations become soft). Similar arguments (Kosterlitz and Thouless 1973) led to the identification of T_2 as the temperature at which vortex–antivortex pairs unbind. Then, if $T_1 < T_2$, we can expect two transitions. For $T_1 < T < T_2$, the interaction potential between vortices recovers its logarithmic dependence on L (as for the 2D-XY model) and we have a KT phase; the second transition, at $T = T_2$, will correspond to the KT transition. If $T_1 \geqslant T_2$ we will have just one transition and both phenomena, walls becoming flexible and vortex-antivortex unbinding, will occur for $T \geqslant T_1$. For the XY-model with symmetry breaking $p = 1$ (corresponding to an in-plane magnetic field), the work of José *et al* (1977) predicts a single crossover temperature ($T_1 = T_2$): in a magnetic field there is no standard phase transition. However, those theoretical results were obtained for the planar-model and could be modified when out-of-plane spin components are included—for instance, an additional anomaly has been noted in the specific heat (Tobochnik and Chester 1979) and static correlation of S_z (Kawabata and Bishop 1982).

4. Numerical simulation and analysis

A combined Monte Carlo (MC)—molecular dynamics (MD) method (Kawabata *et al* 1986) was used to determine the dynamic structure functions $S(q, \omega)$. The simulations
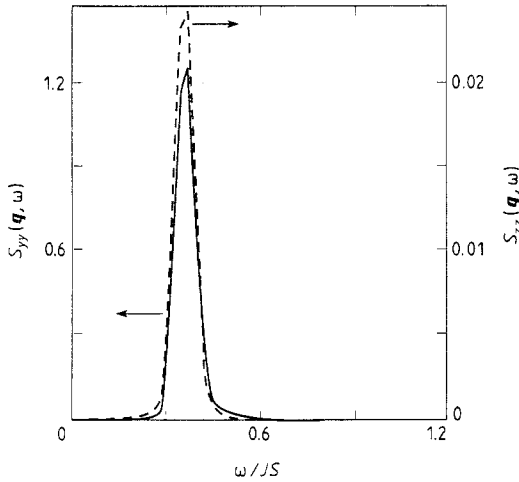
Figure 2. Results for $S_{yy}(q = 0, \omega)$ (full curve) and for $S_{zz}(q = 0, \omega)$ (broken curve) obtained from MC–MD simulations of the Hamiltonian (2.1) on a 100×100 lattice. The plots correspond to $T = 0.7 \, JS^2$.

were performed on a 100×100 square lattice for the model (2.1), with periodic boundary conditions. First, an MC algorithm of 10^4 steps was used to produce three equilibrium configurations at a desired temperature. These configurations are then used as initial conditions for an energy-conserving MD simulation of the equations of motion. The time integration was performed with a standard fourth-order Runge–Kutta method, with a fixed time step of $0.04 \, (JS)^{-1}$. The dynamic structure function $S_{\alpha\alpha}(q, \omega)$ ($\alpha = x, y, z$) was then determined from the Fourier transform of the space- and time-correlation functions, $\langle S_\alpha(0, 0)S_\alpha(r, t)\rangle$. The structure functions resulting from the three initial conditions for a given temperature were then averaged. A smoothing algorithm on $S(q, \omega)$, as in Mertens *et al* (1987), was also employed to reduce the effects of a finite time series and statistical fluctuations.

Simulations were performed for a magnetic field corresponding to $h = 0.05$ and for temperatures in the range $0.7 \, S^2 \leqslant T \leqslant 1.3 \, JS^2$ (in intervals $\Delta T = 0.1 \, JS^2$). For simplicity, we will discuss separately two sets of data: (i) low-temperature data $(0.7 \, JS^2 \leqslant T \leqslant 0.9 \, JS^2)$, and (ii) high-temperature data $(1.0 \, JS^2 \leqslant T \leqslant 1.3 \, JS^2)$.

4.1. Low-temperature data

Here, the yy- and zz-correlation functions show a simple structure (figure 2) consisting of a well defined finite frequency peak at ω_q which softens (i.e., $\omega_q \to 0$) and becomes broader as T increases. This peak can be identified as the one-spin wave peak predicted in (2.3a) and (2.3b). Figure 3 shows the spin wave dispersion obtained from our simulation data at $T = 0.7 \, JS^2$; it compares reasonably well to theory (continuous curve) especially since renormalisation effects due to temperature are not included in (2.4). Evaluating (2.6) at $q = 0$ for $h = 0.05$, we obtain $R(q = 0) \simeq 78$. This number corresponds to a calculation made at $T = 0$ and shows that $I_y(0) \gg I_z(0)$; the difference between y and z intensities decreases as q increases. Using the simulation data, we can estimate $R(q = 0)$ at different temperatures obtaining $R(q = 0) \simeq 51$, 44 and 32 for $T = 0.7 \, JS^2$, $0.8 \, JS^2$ and $0.9 \, JS^2$, respectively. The value obtained for $T = 0.7 \, JS^2$ is comparable to the calculated one($T = 0$). The decreasing of $R(q)$ as T increases is mainly due to the decreasing of $I_y(q)$, since $I_z(q)$ remains roughly constant.
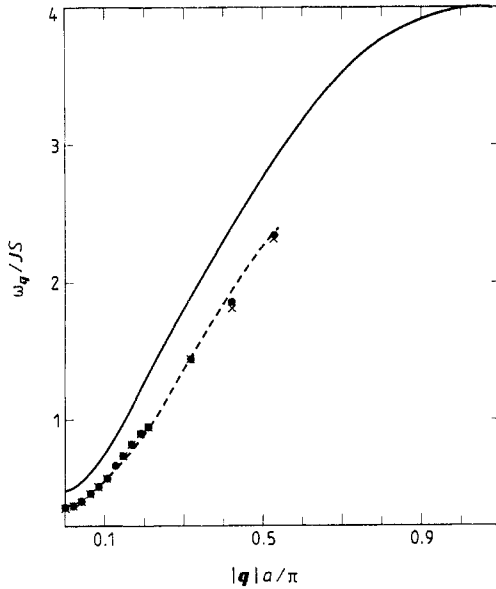
Figure 3. Spin-wave dispersion obtained from the simulated data for wavevectors along the x axis at $T = 0.7 JS^2$. The crosses and circles correspond, respectively, to data taken from $S_{zz}(q, \omega)$ and $S_{yy}(q, \omega)$. The full curve corresponds to equation (2.4).

The Bragg peak predicted in (2.7) is clearly seen in $S_{xx}(q = 0, \omega)$. For small q, $S_{xx}(q, \omega)$ exhibits a central peak and two finite frequency peaks (figure 4) that can be interpreted as due to the sum and difference processes discussed in section 2. Equation (2.11) assures that, for $q \neq 0$, the central peak (discussed below) cannot be produced by difference processes. Figure 5 displays the data obtained for the frequencies of spin-wave difference- (lower data) and sum- (upper data) peaks at $T = 0.7 JS^2$; they fit reasonably well to straight lines, as predicted by (2.12) and (2.13). Notice that the straight lines shown in figure 5 extrapolate to the expected point at $q = 0$, namely, $\omega_D(q = 0) = 0$, and $\omega_S(q = 0) \simeq 0.72 JS$ (from figure 3 we obtain a gap of $0.36 JS$ at $T = 0.7 JS^2$).

It is tempting to suppose that the central peak observed in $S_{xx}(q, \omega)$ (for small q) is related to the presence of domain walls (section 3). Simulation studies performed for 2D-XY models with a 4-fold in-plane symmetry breaking (implying $\pi/2$ domain walls) also show a central peak at low temperatures (Gouvêa *et al* 1989b) and, indeed, scattering from domain walls can be established as a mechanism to produce central peaks. Unfortunately, an analysis of our simulation data—focusing on the central peak behaviour (low T)—and its comparison to a theory including the effects mentioned above (spin waves, domain walls, vortices and their interactions) cannot be done because such theory, to our knowledge, is not available in the literature at the time of writing. Consequently, we cannot be conclusive in asserting that domain walls are responsible for the observed central peak. Our simulation data show that this central peak, or better, its width Γ_x and intensity I_x, suffer a change of behaviour for $T \geqslant 1.0 JS^2$. For $0.7 JS^2 \leqslant T \leqslant 0.9 JS^2$, the width decreases while the intensity increases as T increases; i.e., the central peak becomes narrower and higher as $T \to 1.0 JS^2$. The intensity reaches a local maximum around $T = 1.0 JS^2$. For $T > 1.0 JS^2$, the width does not vary appreciably (we observe a slight increasing) with T and the intensity I_x decreases as T increases. Regarding the $S_{yy}(q, \omega)$ and $S_{zz}(q, \omega)$ correlation functions, a central peak starts developing in the vicinity of $T = 1.0 JS^2$. We interpret these changes as due to a strong crossover occurring about $T_c = 1.0 JS^2$.
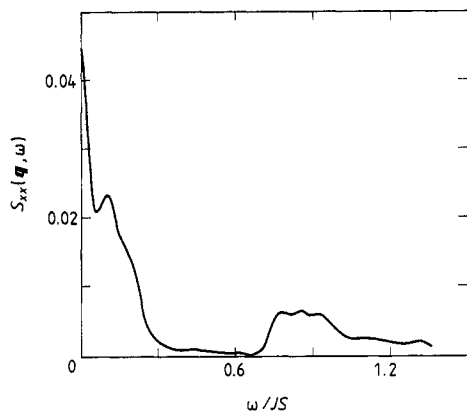
Figure 4. Results for $S_{xx}(q, \omega)$ from MC–MD simulations of the Hamiltonian (2.1) on a 100×100 lattice for $q = (0.06\,\pi, 0)\,a^{-1}$ at $T = 0.7\,JS^2$.
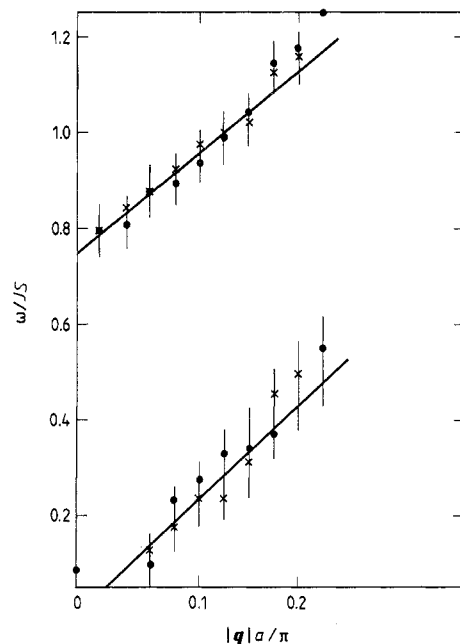
Figure 5. Simulation data for the frequencies ω_D of spin-wave difference (lower data) and ω_S of spin-wave sum (upper data) peaks (as explained in the text). The crosses ($\times$) and circles ($\bullet$) indicate data taken from $S_{xx}(q, \omega)$ for q along the y direction ($\times$) and x-($\bullet$) direction, respectively.

4.2. High-temperature data

As discussed in section 3, we can expect that this crossover will be related to such complex phenomena as vortex-antivortex pair unbinding and domain walls becoming flexible (i.e., $T_c \simeq T_1 \geq T_2$). We also discussed that, in the presence of an in plane magnetic field, the pairs should unbind at a temperature T_c above T_{KT} (which is the transition temperature for the pure XY-model; $T_{KT} \simeq 0.8\,JS^2$)—as observed in the present simulations. The low-temperature data analysis suggests that the $S_{xx}(q, \omega)$ correlation functions will be more sensitive to effects due to domain walls. Therefore, effects due to the unbinding of vortices pairs should be seen more clearly in $S_{yy}(q, \omega)$ and $S_{zz}(q, \omega)$.

Recently, Mertens *et al* (1987, 1989) have proposed a phenomenological theory to explain the dynamic properties of spin vortices in 2D-XY ferromagnets. The theory assumes an ideal gas of unbound vortices above T_{KT} and predicts a central peak for both in- and out-of-plane correlations. For the in-plane central peak, their theory gives

$$\Gamma_y(q) = \tfrac{1}{2}[\pi(\sqrt{2} - 1)]^{1/2}(\bar{v}/\xi)\sqrt{1 + (\xi q)^2} \tag{4.1}$$

for the q-dependent width and

$$I_y(q) = (S^2/4\pi)\,\xi^2/[1 + (\xi q)^2]^{3/2} \tag{4.2}$$

for the integrated intensity, where $\bar{v}$ is the root-mean-square velocity and ξ is the correlation length. The width of the out-of-plane central peak is given by

$$\Gamma_z(q) = \bar{v}q. \tag{4.3a}$$

We will assume, for the moment, that a weak magnetic field does not seriously

compromise the picture of a gas of vortices moving above T_c. In this context, the main effects due to the field would be: (i) to increase the transition temperature, i.e. $T_c > T_{KT}$, and (ii) to increase the average velocity $\bar{v}$ (section 3) with which vortices move in the system. Then, we can compare the predictions of that phenomenological theory with the MC–MD simulation results for $S_{yy}(\boldsymbol{q}, \omega)$ and $S_{zz}(\boldsymbol{q}, \omega)$. The predicted q-dependencies ((4.1), (4.2) and (4.3)) of Γ_z, Γ_y and I_y are well supported by the simulation data (figure 6). Table 1 gives the parameters $\bar{v}$ and ξ obtained by fitting to the width and intensity of the central peaks. The data obtained for Γ_z and Γ_y overestimate the real values due to the difficulty of subtracting the softened spin-wave peak which appears (for small $\boldsymbol{q}$) close to the central peak. Consequently, the values obtained for $\bar{v}$, from fitting to the widths, are also overestimated. Using an equation of motion for free vortices, Huber (1982) obtained an expression for $\bar{v}$ for the 2D-XY model. His formula can be written, approximately (see Mertens *et al* 1989) as

$$\bar{v} = (\sqrt{\pi}/2) \exp(-b/\sqrt{\tau})(b/\sqrt{\tau} + 0.58)^{1/2} \tag{4.3b}$$

where

$$\xi(T) = \xi_0 \exp(b\tau^{-1/2}) \qquad \tau = (T - T_c)/T_c. \tag{4.4}$$

Here ξ_0 is of the order of the lattice constant a and b has been found (Heinekamp and Pelcovitz 1985) to be temperature dependent. Equation (4.3) predicts a strong increase of $\bar{v}$ for temperatures slightly above T_c and a saturation for $\tau \simeq 0.36$. In order to compare the simulation values for $\bar{v}$ to the ones predicted by (4.3), we used $\xi_0 = a$, $T_c = 1.0\,JS^2$ and obtained b by fitting (4.4) to the ξ-values obtained from Γ_y. Obviously, this is an approximate calculation for $\bar{v}$. The values obtained from the simulations compare well with the calculated ones (table 1); notice that the simulation values are larger than the calculated values. We observe that $\bar{v}$ increases with T; probably, in order to achieve the region where $\bar{v}$ remains constant as T increases, we would have to consider still higher temperatures. It is interesting to compare our calculated values for $\bar{v}$, in the presence of a field, to the ones obtained by Mertens *et al* (1989) for $h = 0$ (using (4.3)). The comparison cannot use the absolute temperature T, since T_c is different for the two cases, but can be done in terms of the reduced temperature τ. For $h = 0$, we repeat the values obtained in the referred work to (here the b-values (4.3) were taken from the work by Heinekamp and Pelcovitz (1985)): $\bar{v} = 0.30, 0.47$ and 0.56 for $\tau = 0.125, 0.250$ and 0.375, respectively. The last column in table 1 gives $\bar{v}$ corresponding to $\tau = 0.1, 0.2$ and 0.3, respectively. The immediate conclusion is that the average vortex velocity increases when a magnetic field is applied.

For the 2D-XY model, the (in-plane) spin waves are expected to be strongly softened for $T > T_{KT}$ (Nelson and Kosterlitz 1979); experiments and numerical simulations have checked this behaviour. CoCl$_2$ intercalated into graphite has been taken as an example of 2D-easy plane ferromagnets (Elahy and Dresselhaus 1985). Extensive inelastic neutron scattering experiments (Zabel and Shapiro 1987) have been performed on this compound and a transition is observed at $T_u = 9.6$ K (corresponding to $T_u \simeq 0.9\,JS^2$) which has been tentatively identified as a KT-transition. Also, the temperature dependence of the magnon dispersion was measured and spin waves for $q \geqslant 0.1$ were observed to renormalise continuously while those at small q disappeared at T_u—in qualitative agreement with the predictions of Nelson and Kosterlitz (1979).

The effects of an in-plane field were studied experimentally by Wiesler *et al* (1988). When the field is applied, they observed that, the central peak loses intensity and its width decreases while spin-wave peaks persist for $T > T_u$, even for small q. These authors
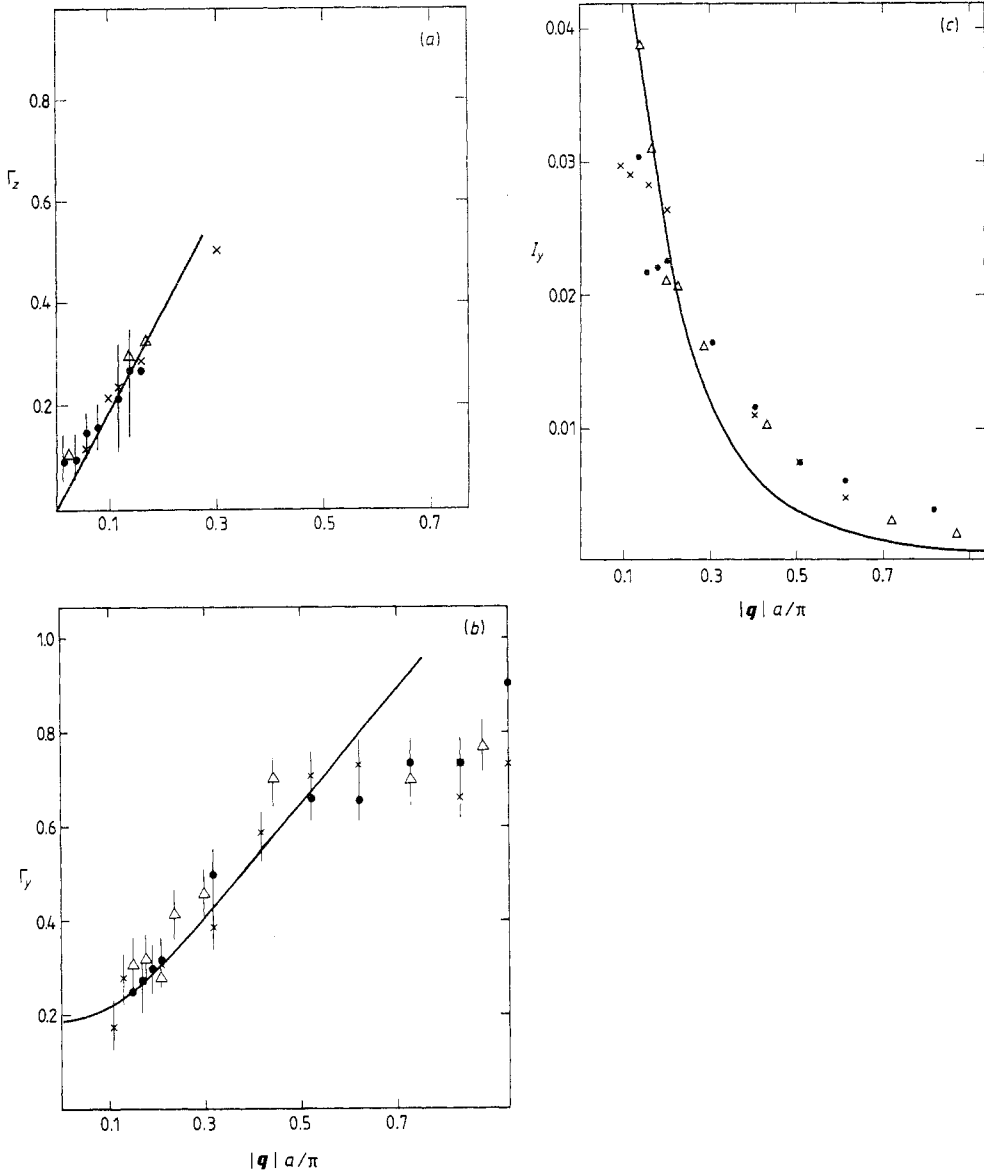
Figure 6. Simulation data at $T = 1.1 JS^2$ for (a) the width Γ_z of the central peak in $S_{zz}(q, \omega)$ ($\bar{v} = 0.60 \pm 0.10$); (b) the width Γ_y ($\xi = 2.2$; $\bar{v} = 0.71$) and (c) intensity I_y of the central peak in $S_{yy}(q, \omega)$ $\xi = 1.6$. Data points for the intensity result from estimating I_y from plots like figure 7 assuming a squared Lorentzian form. Data for three different orientations of q are shown: (●) for q along $[1, 0]$; (×) for q along $[0, 1]$, and (△) for q along $[1, 1]$ directions. Full curves are fits to: (a) (4.3), (b) (4.1), and (c) (4.2) for small q.

concluded that the effect of the field is to effectively raise T_u without softening the spin waves energy. Our numerical simulations ($h = 0.05$) agree qualitatively with these experiments since we obtain a higher transition temperature ($T_c \simeq 1.0 JS^2$ compared to $0.8 JS^2$ for the pure XY-model) when an in-plane magnetic field is applied and we also observe in-plane spin waves for temperatures well above T_c. Figure 7 shows that spin

Table 1. Parameters $\bar{v}$ and ξ obtained by fitting to the intensities and widths of the central peaks in $S_{yy}(q, \omega)$ and $S_{zz}(q, \omega)$ in our MC–MD data for the Hamiltonian (2.1) ($h = 0.05$). The last column gives $\bar{v}$ values obtained from (4.3) and (4.4) using $T_c = 1.0\,JS^2$ and $\xi_0 = a$. For $\xi(T)$, we used the values given in the third column of this table.

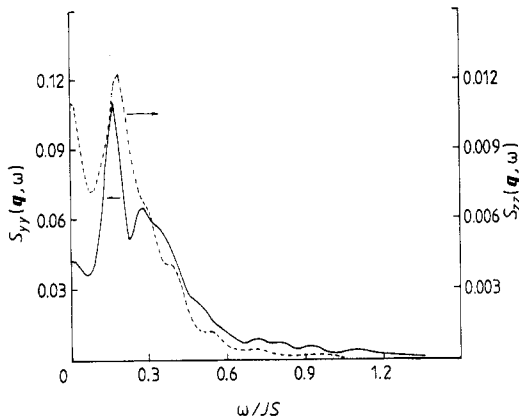| T	$\xi(\Gamma_y)$	$\xi(\Gamma_y)$	$\bar{v}(\Gamma_y)$	$\bar{v}(\Gamma_z)$	$\bar{v}$(from (4.3))
1.1	1.6	2.2	0.71	0.60	0.47
1.2	1.1	2.0	0.71	0.79	0.50
1.3	0.9	1.4	0.74	0.68	0.61

Figure 7. Results from MC–MD simulations for the Hamiltonian (2.1) on a 100×100 lattice for $q = 0.08\,\pi a^{-1}$ at $T = 1.1\,JS^2$ for $S_{yy}(q, \omega)$ (full curve) and $S_{zz}(q, \omega)$ (broken curve).

waves can be clearly seen for both yy- and zz-correlation functions at $T = 1.1\,JS^2$, even for low q. Our interpretation is that, in the presence of a field, the vortex pairs are more tightly bound and the density n_v of free vortices is lower than in the pure 2D-XY model. As a consequence, the correlation length ξ ($n_v \simeq (2\xi)^{-2}$) will be larger, and it is reasonable to have spin waves with wavevectors $q > q_c$ ($q_c \simeq \xi^{-1}$). We observe spin waves with wavevector as small as $q = 0.06\,\pi$ ($T = 1.1\,JS^2$). However, then the values given for ξ in table 1 seem to be too small. The experimentally observed reduction in the width of the in-plane central peak can also be explained by a vortex ideal gas phenomenology (Mertens *et al* 1989). This theory predicts that $\Gamma \propto \bar{v}/\xi$ for small q. Then, from (4.3) and (4.4), we obtain $\Gamma \propto \exp(-2b\tau^{-1/2})$, where we have only kept the exponential dependence on τ because it is dominant. In the presence of a field, the transition temperature is higher, which means that τ will be lower—comparing the same temperature interval above T_c for $h = 0$. A decrease in τ results in a reduction of the width as was observed in the experiments.

An unexpected feature in our simulations is that the out-of-plane spin wave shows a strong softening for $T \geqslant 1.2\,JS^2$ (figure 8). Also, $C_z(q, t = 0) = \int S_{zz}(q, \omega)\,d\omega$, which is related to the susceptibility, shows a maximum at $T = 1.2\,JS^2$. These features indicate that a dynamical crossover (or a transition; we cannot distinguish these alternatives with our numerical accuracy), closely related to the z-spin component, takes place at this temperature. Presently, we have no explanation for this behaviour, but we note that it occurs at the same temperature (relative to T_c) where specific heat and S_z correlations
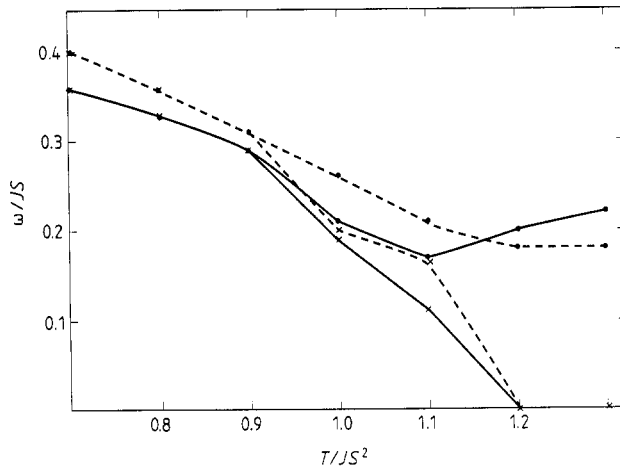
Figure 8. Spin-wave frequencies (from our simulations) as functions of temperature determined from $S_{yy}(q, \omega)$ (●) and $S_{zz}(q, \omega)$ (×) for two wavevectors: $q = 0$ (full curve) and $q = 0.04 \, \pi a^{-1} e_x$ (broken curve).

showed an anomaly for the zero-field case (Tobochnik and Chester 1979, Kawabata and Bishop 1982).

5. Conclusions

In this paper, we have studied the effects of an in-plane magnetic field on 2D-XY spin systems. In the absence of a field, vortices are well known as important excitations in describing the properties of 2D-XY models. An external (in-plane) magnetic field, breaks the rotational symmetry of the XY-plane and, therefore, influences the vortex shape and behaviour. Besides, a field can introduce domain walls corresponding to a 2π-rotation about the privileged direction (here the x-axis). Our approximate analytical treatment and numerical simulations (section 3) show how the shape of the *single* vortex changes and how it moves in the presence of the field. The simulations suggest that vortex *pairs* will be connected by domain walls; the 2π-walls can be thought of as consisting of two π-walls separated by a narrow domain (of width $\sim$ the vortex diameter) where the spins are antiparallel to the field.

The MC–MD data (section 4) for temperatures lower than $1.0 \, JS^2$ are well interpreted within a spin-wave approximation (section 2), provided two-spin-wave processes are included. However, an anomalous central peak is observed in the $S_{xx}(q, \omega)$ correlation function at all temperatures ($0.7 \, JS^2 \leqslant T \leqslant 1.3 \, JS^2$) we have considered in the simulations. Our hypothesis is that this central peak is intimately related to the presence of domain walls but additional theoretical work is necessary in order to confirm this possibility since many mechanisms can contribute to a central peak. The data analysis concerning this central peak in $S_{xx}(q, \omega)$ reveals a change taking place at about $T = 1.0 \, JS^2$: for $0.7 \, JS^2 \leqslant T \leqslant 1.0 \, JS^2$, this central peak becomes narrower and more intense as T increases, while for $T \geqslant 1.0 \, JS^2$ it loses intensity and becomes slightly broader. Simultaneously, changes are also observed in the yy- and zz-correlation functions where central peaks are seen to develop for $T \geqslant 1.0 \, JS^2$. We interpret these changes as due to a strong crossover from magnetic field to vortex symmetry at $T_c \simeq 1.0 \, JS^2$.

For the pure 2D-XY model, a topological phase transition due to the unbinding of vortex pairs occurs at $T_{KT} \simeq 0.8\,JS^2$. Since the magnetic field used in our simulations is small ($h = 0.05$, $H \ll J$), we do not expect it to drastically alter the properties of the system. Therefore, we expect that the crossover at $T_c = 1.0\,JS^2$ is induced by the unbinding of pairs of vortices although domain walls should also play a relevant role. It is reasonable to have $T_c > T_{KT}$ because, in a magnetic field, a pair of vortices is more tightly bound and will unbind at a higher temperature. Our data suggest that effects related to the existence of domain walls are more important for $S_{xx}(\boldsymbol{q}, \omega)$ functions; $S_{yy}(\boldsymbol{q}, \omega)$ and $S_{zz}(\boldsymbol{q}, \omega)$ would then be more sensitive to *vortices*. With this thought in mind, the central peaks in yy- and zz-correlation functions (for $T \geq 1.0\,JS^2$), specifically their widths and intensities as taken from our simulations, were analysed and compared to the predictions of a phenomenological theory based on a free vortex gas picture. The agreement is quite good and provides evidence for vortex diffusion above T_c.

Our results were compared with recent inelastic neutron scattering experimental data (Wiesler *et al* 1988) for $CoCl_2$–GIC with an in-plane magnetic field and the qualitative agreement is very good. Unfortunately, these experiments did not separately measure the out-of-plane contribution and, as yet, have not been taken to temperatures as high as $T^* = 1.2\,JS^2$ ($\simeq 13$ K). Thus, our results (from simulations) revealing a softening of out-of-plane spin waves for $T \geq 1.2\,JS^2$ and possibly a strong second anomaly at T^* cannot yet be compared with experiment. To understand this interesting high temperature region requires more theoretical and experimental studies.

Acknowledgments

References

Amit D J, Goldschmidt Y Y and Grinstein S 1980 *J. Phys. A: Math. Gen.* **13** 583
Cotê R and Griffin A 1986 *Phys. Rev.* B **34** 6240
Einhorn M B, Savit R and Ravinovici E 1980 *Nuclear Phys.* B **170** 16
Elahy M and Dresselhaus G 1985 *Phys. Rev.* B **30** 7225
Gouvêa M E, Wysin G M, Bishop A R and Mertens F G 1989a *Phys. Rev.* B **39** 840
Gouvêa M E, Wysin G M, Bishop A R and Mertens F G 1989b *J. Phys.: Condens. Matter* to be published
Heilmann J U, Kjems J K, Endoh Y, Reiter G R, Shirane G and Birgeneau R J 1981 *Phys. Rev.* B **24** 3939
Heinekamp S W and Pelcovitz R A 1985 *Phys. Rev.* B **32** 4258
Huber D L 1982 *Phys. Rev.* B **26** 3758
Hudák O 1982 *Phys. Lett.* **82A** 245
José J V, Kadanoff L P, Kirkpatrick S and Nelson D R 1977 *Phys. Rev.* B **16** 1217
Kawabata C and Bishop A R 1982 *Solid State Commun.* **42** 595
Kawabata C, Takeuchi M and Bishop A R 1986 *J. Magn. Magn. Mater.* **54–57** 871
Kosterlitz J M and Thouless D J 1973 *J. Phys. C: Solid State Phys.* **6** 1181
Lee D H and Grinstein G 1985 *Phys. Rev. Lett.* **55** 541
Mertens F G, Bishop A R, Wysin G M and Kawabata C 1987 *Phys. Rev. Lett.* **59** 117
Mertens F G, Bishop A R, Wysin G M and Kawabata C 1989 *Phys. Rev.* B **39** 591
Nelson D R and Fisher D S 1977 *Phys. Rev.* B **16** 4945

Nelson D R and Kosterlitz J M 1979 *Phys. Rev. Lett.* **39** 1201
Tang S and Mahanti S D 1986 *Phys. Rev.* B **33** 3419
Tobochnik J and Chester G V 1979 *Phys. Rev.* B **20** 3761
Wiesler D G, Zabel H and Shapiro S M 1988 Preprint
Zabel H and Shapiro S M 1987 *Phys. Rev.* B **36** 7292